

LA-JR-020510

Approved for public release;
distribution is unlimited.

Title: C5G7 MOX BENCHMARK PROBLEMS RESULTS FROM
THE PARTISN TRANSPORT CODE

Author(s):

J. A. DAHL, CCS-4
R. E. ALCOUFFE, CCS-4

Submitted to:
Expert Group on 3-D Radiation Transport Benchmarks
Nuclear Energy Agency

Los Alamos

NATIONAL LABORATORY

Los Alamos National Laboratory, an affirmative action/equal opportunity employer, is operated by the University of California for the U.S. Department of Energy under contract W-7405-ENG-36. By acceptance of this article, the publisher recognizes that the U.S. Government retains a nonexclusive, royalty-free license to publish or reproduce the published form of this contribution, or to allow others to do so, for U.S. Government purposes. Los Alamos National Laboratory requests that the publisher identify this article as work performed under the auspices of the U.S. Department of Energy. Los Alamos National Laboratory strongly supports academic freedom and a researcher's right to publish; as an institution, however, the Laboratory does not endorse the viewpoint of a publication or guarantee its technical correctness.

C5G7 MOX Benchmark Problem Results From the PARTISN Transport Code

Jon A. Dahl and Raymond E. Alcouffe
Transport Methods Group
Los Alamos National Laboratory
Los Alamos, NM 87545

Introduction

In early 2001 the Expert Group on 3-D Radiation Transport Benchmarks of the Nuclear Energy Agency solicited participants for a proposed new benchmark [1]. The benchmark, known as C5G7 MOX, is intended to be a basis to measure current transport code abilities in the treatment of reactor core problems without spatial homogenization. We have participated with the code transport code PARTISN [2]. PARTISN (PARallel Time Dependent SN), PARTISN solves the linear Boltzmann transport equation in static and time dependent forms on one, two and three dimensional orthogonal grids using the deterministic (S_N) method. A variety of spatial discretization methods are incorporated into PARTISN, however all calculations performed here used the diamond difference approach, coupled with a volume fraction method for non-Cartesian problem geometries. Acceleration of the source iterations is accomplished with diffusion synthetic acceleration (DSA).

Description of Work

For the two dimensional C5G7 MOX problem we used an X-Y Cartesian grid. Rather than creating a “stair stepped” grid to represent each fuel pin, we began with an unstructured quadrilateral grid created using ICEM CFD Engineering grid generation tools. This unstructured grid more closely represents the actual geometry of each water channel-fuel pin combination. We then overlay a Cartesian mesh onto the unstructured grid and calculate to volume fractions of each material where a Cartesian mesh cells is intersected by an unstructured mesh material boundary. This methodology allows the preservation of mass without changing the density in cells which are not intersected by actual material interfaces. We generated three grids for the two dimensional case, a coarse, medium, and fine, corresponding to a 5x5, 10x10 and 15x15 grid in each water channel-fuel pin cell, and 30 mesh cells in each direction of the water reflector. An example of the medium mesh grid in a typical water channel-fuel pin region can be found in figure 1. The cells containing an X indicate mesh cells where volume fractions of fuel and water have been calculated. The unmarked cells contain just one material, either the appropriate water or fuel.

The grid for the three dimensional problem was generated in the same way, beginning with a three dimensional unstructured mesh and calculating the corresponding volume fractions for Cartesian X-Y-Z mesh cells intersecting material interfaces. We performed calculations on two three dimensional grids, one coarse and one medium, which, as in the two dimensional case, contained 5x5 and 10x10 mesh cells respectively, in each water

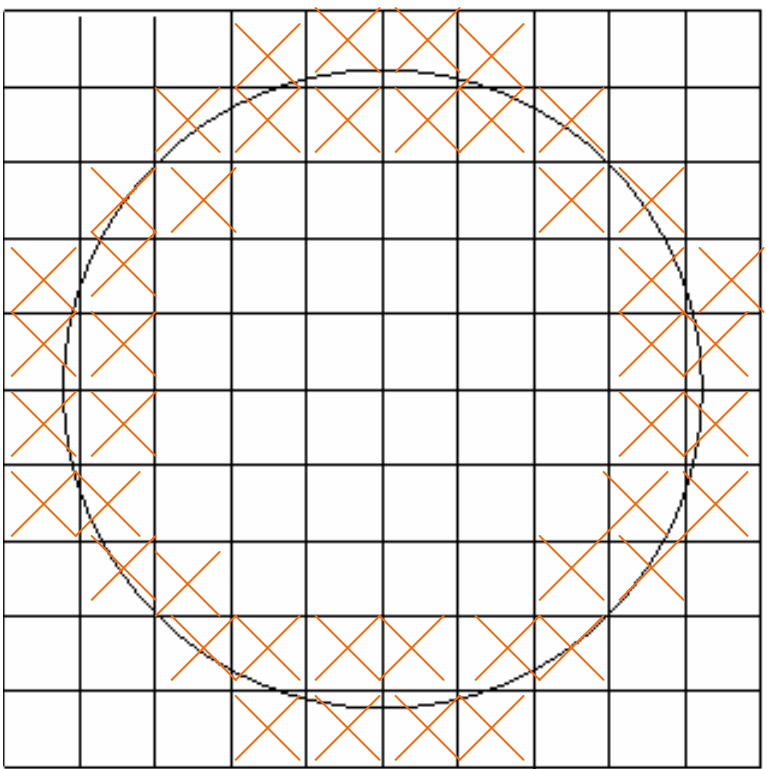


Figure 1 – Representation of fuel pin meshing

channel-fuel pin cell, and 30 mesh cells in each direction of the water reflector. The coarse mesh fuel region contained 20 cells in the Z direction, for a total of 200x200x50 or 6 million cells. The fuel region of the medium mesh was comprised of 50 cells in the Z direction for a total of 370x370x80, or 10,952,000 cells. A fine three dimensional mesh we also generated, consisting of 17,496,000 cells, but two dimensional convergence studies indicated that a mesh this fine is not required.

We ran each problem using the square Tchebechev-Legendre quadrature set [3] and diamond difference spatial differencing. The pointwise fluxes were converged to an error of 1.0E-05. The diffusion equations for the DSA were solved using a parallel multigrid technique described by Alcouffe [4]. Varying S_N orders for each mesh were run to determine that spatial and angular convergence was achieved.

Both the two and three dimensional problems were run on the Bluemountain computer, located at the Los Alamos National Laboratory. Bluemountain consists of 48 SGI Origin 2000 boxes with 128 processors each. The two dimension problems were run with 16 processors, while the three dimensional problems were run with 126 to 768 processors, depending on mesh size and S_N order.

Computational Results

For this benchmark, we report the eigenvalues and pin powers for the medium mesh grids run with S_{26} square Legendre-Tchebychev quadrature. Table 1 presents the eigenvalues for both the two and three dimensional cases.

Table 1: k Eigenvalues for 2-D/3-D C5G7 MOX Benchmark Problems

Dimension	k Eigenvalue
2-D	1.18637
3-D	1.18362

In Table 3, the normalized minimum and maximum pins powers for the two dimensional coarse and medium mesh and the three dimensional coarse mesh are shown. These results were also generated with a quadrature order of S_{26} . Complete pin power results can be found in tables 3 – 7.

Table 2: Maximum and Minimum Normalized Pin Powers for 2-D/3-D C5G7 MOX Benchmark Problem

Mesh	Maximum	Minimum
2-D Medium Mesh	2.5025	0.2319
3-D Medium Mesh	2.5018	0.2318

Table 3 – 2-D UO₂ Pin Powers near Axis of Symmetry

	1	2	3	4	5	6	7	8	9	10	11	12	13	14	15	16	17		
1	2.0829	2.1399	2.1888	2.2155	2.2264	2.2307	2.1875	2.1508	2.1230	2.0586	2.0024	1.9518	1.8583	1.7559	1.6341	1.4857	1.2810	1	
2		2.1790	2.2238	2.2699	2.3035	2.3746	2.2577	2.2175	2.2540	2.1232	2.0657	2.0773	1.9233	1.7985	1.6561	1.4941	1.2811	2	
3			2.3052	2.4417	2.4737		2.3872	2.3398		2.2416	2.1822		2.0657	1.9343	1.7147	1.5134	1.2851	3	
4				2.5025	2.4599	2.2994	2.2498	2.2962	2.1542	2.1025	2.1492	2.0844		1.8166	1.5416	1.2926		4	
5					2.4069	2.4322	2.2834	2.2363	2.2827	2.1416	2.0885	2.1261	2.0061	1.9780	1.8367	1.5638	1.2971		5
6						2.3524	2.3062		2.2103	2.1519		2.0309	1.9434		1.6153	1.3008			6
7						2.2226	2.1822	2.2300	2.0910	2.0355	2.0605	1.9076	1.8187	1.7716	1.5338	1.2761		7	
8							2.1440	2.1906	2.0551	2.0002	2.0223	1.8709	1.7821	1.7392	1.5092	1.2573		8	
9								2.1019	2.0445			1.9140	1.8216		1.5412	1.2458			9
10									1.9716	1.9198	1.9431	1.7978	1.7137	1.6748	1.4538	1.2120		10	
11										1.8708	1.8948	1.7571	1.6777	1.6369	1.4208	1.1850		11	
12											1.7941	1.7207			1.4398	1.1635			12
13												1.6961	1.6773	1.5670	1.3399	1.1166			13
14													1.4794	1.2635	1.0675				14
15														1.3205	1.1768	1.0128			15
16															1.0812	0.9534			16
17																0.8770			17

Table 4 - 2-D UO₂ Pin Powers near Water Reflector

UO₂-2 Normalized Pin Powers

	18	19	20	21	22	23	24	25	26	27	28	29	30	31	32	33	34		
18	0.7936	0.7896	0.7714	0.7501	0.7253	0.6995	0.6589	0.6212	0.5873	0.5444	0.5052	0.4702	0.4290	0.3941	0.3734	0.3901	0.5025	18	
19		0.8271	0.8317	0.8262	0.8117	0.8088	0.7402	0.6977	0.6806	0.6133	0.5693	0.5475	0.4863	0.4425	0.4140	0.4247	0.5293	19	
20			0.8653	0.9003	0.8877		0.8018	0.7541		0.6652	0.6172		0.5373	0.4896	0.4403	0.4389	0.5355	20	
21					0.8928	0.8521	0.7691	0.7236	0.7100	0.6382	0.5947	0.5815	0.5409		0.4656	0.4443	0.5318	21	
22						0.8404	0.8251	0.7496	0.7069	0.6937	0.6246	0.5820	0.5667	0.5139	0.4936	0.4637	0.4425	0.5217	22
23							0.7532	0.7110		0.6303	0.5860		0.5095	0.4736		0.4449	0.5079	23	
24								0.6898	0.6533	0.6434	0.5793	0.5395	0.5233	0.4656	0.4318	0.4258	0.4122	0.4852	24
25									0.6198	0.6101	0.5504	0.5127	0.4964	0.4417	0.4092	0.4039	0.3923	0.4624	25
26										0.5433	0.5053		0.4363	0.4029		0.3849	0.4401	26	
27											0.4900	0.4567	0.4432	0.3940	0.3651	0.3611	0.3501	0.4124	27
28												0.4262	0.4133	0.3685	0.3420	0.3373	0.3272	0.3853	28
29													0.3602	0.3349		0.3155	0.3595	29	
30														0.3266	0.3132	0.2961	0.2817	0.3295	30
31															0.2705	0.2560	0.3014	31	
32																0.2417	0.2360	0.2778	32
33																0.2319	0.2667	33	
34																	0.2878	34	

Table 5 - 2-D MOX Pin Powers

MOX Normalized Pin Powers

	18	19	20	21	22	23	24	25	26	27	28	29	30	31	32	33	34	
1	1.3138	1.0614	0.9356	0.8632	0.8112	0.7672	0.7118	0.6623	0.6194	0.5688	0.5232	0.4831	0.4370	0.3974	0.3762	0.4086	0.6002	1
2	1.2966	1.3434	1.1704	1.0927	1.0478	1.0446	0.9182	0.8499	0.8385	0.7324	0.6718	0.6565	0.5663	0.5032	0.4689	0.5154	0.5922	2
3	1.2902	1.3205	1.1770	1.1744	1.1188		0.9489	0.8686		0.7545	0.6873		0.6061	0.5412	0.4738	0.5066	0.5883	3
4	1.2923	1.3323	1.2621		1.1116	1.1271	0.9566	0.8794	0.8752	0.7583	0.6971	0.7018	0.5878		0.5122	0.5119	0.5876	4
5	1.2951	1.3594	1.2889	1.1810	1.1438	1.0824	0.9272	0.8538	0.8517	0.7367	0.6764	0.6765	0.6097	0.5370	0.5169	0.5225	0.5878	5
6	1.2965	1.4249		1.2792	1.1415		0.9834	0.9005		0.7841	0.7127		0.6192	0.5760		0.5489	0.5877	6
7	1.2741	1.3329	1.2223	1.1462	1.0367	1.0355	0.8988	0.8314	0.8320	0.7187	0.6584	0.6524	0.5601	0.5205	0.4869	0.5135	0.5810	7
8	1.2559	1.3119	1.1981	1.1226	1.0171	1.0164	0.8854	0.8204	0.8204	0.7098	0.6501	0.6426	0.5514	0.5116	0.4789	0.5074	0.5757	8
9	1.2431	1.3619		1.1887	1.0723		0.9424	0.8670		0.7569	0.6873		0.5884	0.5398		0.5307	0.5723	9
10	1.2120	1.2687	1.1624	1.0888	0.9876	0.9898	0.8618	0.7993	0.8013	0.6929	0.6351	0.6290	0.5393	0.5005	0.4694	0.4969	0.5637	10
11	1.1861	1.2434	1.1410	1.0738	0.9742	0.9740	0.8486	0.7870	0.7881	0.6827	0.6267	0.6210	0.5343	0.4972	0.4652	0.4916	0.5570	11
12	1.1643	1.2860		1.1617	1.0417		0.9041	0.8312		0.7276	0.6632		0.5781	0.5385		0.5150	0.5520	12
13	1.1216	1.1873	1.1347	1.0410	1.0143	0.9676	0.8317	0.7695	0.7718	0.6690	0.6163	0.6189	0.5581	0.4921	0.4758	0.4814	0.5416	13
14	1.0777	1.1250	1.0787		0.9621	0.9811	0.8380	0.7752	0.7752	0.6749	0.6234	0.6299	0.5296		0.4640	0.4642	0.5324	14
15	1.0356	1.0829	0.9845	0.9966	0.9579		0.8237	0.7602		0.6677	0.6120		0.5443	0.4881	0.4282	0.4570	0.5278	15
16	1.0062	1.0911	0.9847	0.9406	0.9155	0.9219	0.8191	0.7651	0.7596	0.6689	0.6175	0.6058	0.5261	0.4699	0.4386	0.4774	0.5361	16
17	1.0135	0.9092	0.8546	0.8184	0.7865	0.7555	0.7101	0.6680	0.6305	0.5840	0.5412	0.5030	0.4582	0.4194	0.3968	0.4203	0.5771	17

Table 6 - 3-D UO₂ Pin Powers near Axis of Symmetry

	1	2	3	4	5	6	7	8	9	10	11	12	13	14	15	16	17		
1	2.0827	2.1396	2.1884	2.2150	2.2258	2.2302	2.1870	2.1503	2.1226	2.0582	2.0020	1.9514	1.8580	1.7556	1.6339	1.4856	1.2811	1	
2		2.1786	2.2233	2.2694	2.3028	2.3741	2.2571	2.2170	2.2534	2.1227	2.0651	2.0768	1.9229	1.7982	1.6559	1.4940	1.2812	2	
3			2.3046	2.4410	2.4731			2.3866	2.3392		2.2411	2.1817		2.0652	1.9340	1.7145	1.5133	1.2851	3
4				2.5018	2.4592	2.2988	2.2493	2.2956	2.1536	2.1019	2.1487	2.0839			1.8163	1.5415	1.2926	4	
5					2.4062	2.4314	2.2827	2.2358	2.2821	2.1410	2.0881	2.1256	2.0057	1.9776	1.8364	1.5637	1.2971	5	
6						2.3519	2.3056		2.2097	2.1514			2.0304	1.9430		1.6151	1.3008	6	
7						2.2220	2.1817	2.2295	2.0904	2.0350	2.0600	1.9072	1.8183	1.7714	1.5338	1.2761	7		
8							2.1434	2.1901	2.0545	1.9996	2.0217	1.8706	1.7819	1.7390	1.5091	1.2573	8		
9								2.1013	2.0441			1.9135	1.8212			1.5411	1.2459	9	
10									1.9710	1.9193	1.9426	1.7974	1.7134	1.6745	1.4537	1.2120	10		
11										1.8704	1.8944	1.7567	1.6774	1.6366	1.4207	1.1850	11		
12											1.7937	1.7204			1.4398	1.1636	12		
13												1.6957	1.6770	1.5667	1.3398	1.1166	13		
14													1.4792	1.2634	1.0675		14		
15														1.3205	1.1768	1.0129	15		
16															1.0813	0.9536	16		
17																0.8771	17		

Table 7 – 3-D UO₂ Pin Powers near Water Reflector

	18	19	20	21	22	23	24	25	26	27	28	29	30	31	32	33	34	18
18	0.7937	0.7898	0.7715	0.7502	0.7254	0.6996	0.6590	0.6213	0.5874	0.5444	0.5053	0.4703	0.4291	0.3942	0.3734	0.3900	0.5022	18
19		0.8272	0.8319	0.8263	0.8118	0.8088	0.7403	0.6977	0.6806	0.6133	0.5693	0.5475	0.4863	0.4425	0.4140	0.4246	0.5290	19
20			0.8653	0.9003	0.8877		0.8017	0.7541		0.6652	0.6172		0.5373	0.4895	0.4403	0.4388	0.5351	20
21				0.8928	0.8520	0.7690	0.7236	0.7100	0.6382	0.5947	0.5814	0.5409		0.4654	0.4441	0.5315	21	
22					0.8403	0.8250	0.7495	0.7068	0.6936	0.6245	0.5819	0.5666	0.5138	0.4935	0.4635	0.4422	0.5213	22
23						0.7532	0.7109		0.6302	0.5859		0.5095	0.4735		0.4447	0.5075	23	
24						0.6897	0.6532	0.6433	0.5792	0.5394	0.5232	0.4655	0.4316	0.4257	0.4120	0.4849	24	
25							0.6197	0.6100	0.5503	0.5127	0.4963	0.4417	0.4092	0.4039	0.3921	0.4620	25	
26								0.5433	0.5053		0.4362	0.4028		0.3848	0.4398	26		
27									0.4899	0.4567	0.4431	0.3939	0.3650	0.3610	0.3500	0.4120	27	
28										0.4261	0.4132	0.3684	0.3419	0.3371	0.3270	0.3850	28	
29											0.3601	0.3348		0.3153	0.3592	29		
30											0.3265	0.3131	0.2960	0.2815	0.3292	30		
31												0.2704	0.2559	0.3011	31			
32												0.2416	0.2360	0.2775	32			
33													0.2318	0.2665	33			
34														0.2875	34			

Table 8 - 3-D MOX Pin Powers

	18	19	20	21	22	23	24	25	26	27	28	29	30	31	32	33	34	
1	1.3139	1.0617	0.9359	0.8634	0.8115	0.7674	0.7121	0.6626	0.6197	0.5691	0.5235	0.4833	0.4372	0.3976	0.3764	0.4087	0.5999	1
2	1.2967	1.3436	1.1707	1.0931	1.0481	1.0449	0.9186	0.8503	0.8389	0.7328	0.6721	0.6568	0.5665	0.5033	0.4691	0.5154	0.5920	2
3	1.2903	1.3207	1.1772	1.1747	1.1191		0.9493	0.8690		0.7548	0.6877		0.6064	0.5414	0.4740	0.5068	0.5880	3
4	1.2924	1.3325	1.2624		1.1120	1.1274	0.9569	0.8798	0.8756	0.7587	0.6975	0.7022	0.5880		0.5124	0.5120	0.5874	4
5	1.2951	1.3595	1.2891	1.1813	1.1441	1.0829	0.9276	0.8542	0.8521	0.7370	0.6768	0.6768	0.6099	0.5372	0.5171	0.5225	0.5876	5
6	1.2966	1.4251		1.2796	1.1419		0.9838	0.9009		0.7845	0.7131		0.6194	0.5763		0.5489	0.5876	6
7	1.2742	1.3331	1.2225	1.1464	1.0372	1.0359	0.8991	0.8317	0.8324	0.7190	0.6587	0.6528	0.5603	0.5208	0.4871	0.5135	0.5808	7
8	1.2560	1.3120	1.1985	1.1230	1.0174	1.0168	0.8858	0.8208	0.8208	0.7101	0.6505	0.6430	0.5517	0.5118	0.4791	0.5074	0.5755	8
9	1.2433	1.3621		1.1891	1.0726		0.9427	0.8674		0.7573	0.6878		0.5887	0.5401		0.5307	0.5721	9
10	1.2121	1.2689	1.1627	1.0892	0.9879	0.9901	0.8622	0.7997	0.8017	0.6932	0.6354	0.6293	0.5396	0.5008	0.4695	0.4969	0.5634	10
11	1.1862	1.2436	1.1412	1.0742	0.9746	0.9743	0.8490	0.7873	0.7884	0.6831	0.6270	0.6214	0.5345	0.4974	0.4653	0.4916	0.5568	11
12	1.1645	1.2863		1.1621	1.0420		0.9044	0.8316		0.7279	0.6636		0.5782	0.5388		0.5150	0.5518	12
13	1.1217	1.1874	1.1350	1.0413	1.0147	0.9679	0.8320	0.7698	0.7721	0.6693	0.6166	0.6191	0.5582	0.4923	0.4759	0.4814	0.5414	13
14	1.0779	1.1252	1.0789		0.9625	0.9814	0.8383	0.7756	0.7755	0.6752	0.6236	0.6301	0.5297		0.4641	0.4643	0.5322	14
15	1.0357	1.0831	0.9848	0.9969	0.9582		0.8240	0.7605		0.6679	0.6122		0.5444	0.4883	0.4282	0.4570	0.5275	15
16	1.0063	1.0913	0.9849	0.9408	0.9158	0.9222	0.8194	0.7653	0.7598	0.6691	0.6178	0.6060	0.5262	0.4700	0.4386	0.4773	0.5359	16
17	1.0136	0.9094	0.8548	0.8185	0.7867	0.7556	0.7102	0.6681	0.6307	0.5841	0.5414	0.5032	0.4583	0.4195	0.3968	0.4202	0.5769	17

Acknowledgements

We wish to thank Todd Wareing for generating the unstructured quadrilateral grid with ICEM CFD Engineering software.

This work was performed under the auspices of the Department of Energy.

References

1. E.E. Lewis, et. Al., "Benchmark Specification for Deterministic 2-D/3-D MOX Fuel Assembly Transport Calculations Without Spatial Homogenization," Nuclear Energy Agency, Nuclear Science Committee, Expert Group on 3-D Radiation Transport Benchmarks Report, NEA/NSC/DOC(2001)17, (2001).
2. R. E. Alcouffé, R. S. Baker, J. A. Dahl, and S. A. Turner, "PARTISN Code Abstract," Physor 2000 International Topical Meeting, Advances in Reactor Physics and Mathematics and Computation into the Next Millennium, Pittsburgh, (2000).
3. R. D. O'Dell, R. E. Alcouffe, "Transport Calculations for Nuclear Analysis: Theory and Guidelines for Effective Use of Transport Codes, LA-10983-MS, Los Alamos National Laboratory, September 1987.
4. R.E. Alcouffe, "A Parallel Multigrid Method for Inversion of the Diffusion Operator in Neutronics Applications," Proceedings ANS International Meeting on Mathematical Methods for Nuclear Applications, Salt Lake City, UT, September (2001).